Glow-Discharge-Induced Sublimation of Polyimide Precursor Monomers: A Systematic Study

Gianluigi Maggioni,*[,†,‡] Alberto Quaranta,[†,‡] Enrico Negro,[†,‡] Sara Carturan,[†,§] and Gianantonio Della Mea[†,‡]

Istituto Nazionale di Fisica Nucleare, Laboratori Nazionali di Legnaro, Viale dell'Università 2, 35020 Legnaro, Padova, Italy, and Department of Materials Engineering and Industrial Technologies, University of Trento, via Belenzani, 12 38100 Trento, Italy

Received July 31, 2003. Revised Manuscript Received January 15, 2004

Glow-discharge-induced sublimation (GDS) is used to deposit thin films of polyimide precursor monomers, i.e., 2,4,6-trimethyl *m*-phenylenediamine (TMPD), 4,4′-hexafluoroisopropylidene dianiline (6FDAm), 3,3′-diaminodiphenyl sulfone (DDS), 4,4′-hexafluoroisopropylidene diphthalic anhydride (6FDA), and 3,3′,4,4′-biphenyltetracarboxylic acid dianhydride (BPDA). Monomer films are also deposited by vacuum evaporation (VE) for the sake of comparison. In situ mass spectrometry points out both the sublimation of integer monomer molecules and the presence of molecular fragments in the glow discharge. AFM images of the film surfaces indicate that GDS allows obtention of smoother surfaces with respect to VE for most of the monomers. FT-IR analysis and UV−Vis fluorescence spectroscopy show that the deposition of integer monomer molecules onto the substrate and the partial incorporation of molecular fragments take place. In particular, the fluorescence features of GDS samples are different from those of VE samples and depend on the incorporated molecular fragments whose optical properties are similar to those of amorphous hydrogenated carbon structures.

1. Introduction

Polyimide thin films are currently used for several applications owing to their excellent physical properties with respect to those of other polymers.[1] Mechanical properties, chemical durability, thermal stability, and the low dielectric constant of polyimides led to their employment in microelectronics and optoelectronics applications.[2,3] Moreover, their resistance under ion beam irradiation has attracted interest for applications in organic scintillator materials for radiation detectors. For this purpose, polymide films doped with fluorescent organic dyes have been produced, and their radiation hardness and scintillation yield have been studied.[4,5]

Vacuum deposition processes, including vapor deposition polymerization[6] (VDP) and ionized cluster beam deposition,[7] have been developed as alternatives to the traditional liquid solution film formation to obtain better thickness control and homogeneity and superior electrical properties by avoiding the use of organic solvents. Recently, a glow-discharge-based deposition technique has been developed for the realization of organic coatings.[8,9] This method, which is named glow-discharge-induced sublimation (GDS), is based on a plasma-induced sublimation process, promoted by a weakly ionized gas discharge produced in RF magnetron sputtering equipment. Low-energy (E < 500 eV) ions impinge on the solid organic precursors, e.g. pyromellitic dianhydride (PMDA) and 4,4′-oxydianiline (ODA), leading to the sublimation of the organic molecules and to their condensation onto the substrate. FT-IR analyses performed on the films revealed that the as-deposited coatings mainly consist of a mixture of polyamic acid and nonreacted monomers, whose polymerization can be completed only after curing. PMDA−ODA films deposited by the GDS method exhibit higher adhesion to the substrate than the VDP films.[10] This feature arises from the higher average energy of the monomer admolecules in the GDS process (some eVs) as compared to VDP (less than one eV) as well as from the presence of highly reactive chemical species such as radicals produced by the monomer/plasma interactions which promote the film/substrate chemical interaction.

* To whom correspondence should be addressed. E-mail: maggioni@lnl.infn.it.

† Istituto Nazionale di Fisica Nucleare.

‡ Department of Materials Engineering and Industrial Technologies, University of Trento.

§ Department of Physics, University of Trento.

(1) Sazanov, Yu. N. *Russ. J. Appl. Chem.* **2001**, *74*, 1253.
(2) Opila, R. L.; Eng, J. *Prog. Surf. Sci.* **2002**, *69*, 125.
(3) Ma, H.; Jen, A. K. Y.; Dalton, L. R. *Adv. Mater.* **2002**, *14*, 1339.
(4) Quaranta, A.; Carturan, S.; Maggioni, G.; Della Mea, G.; Ischia, M.; Campostrini, R. *Appl. Phys. A.* **2001**, *72*, 671.
(5) Quaranta, A.; Vomiero, A.; Carturan, S.; Maggioni, G.; Della Mea, G. *Synth. Met.* **2003**, *138*, 275.
(6) Takahashi, Y.; Iijima, M.; Inagawa, K.; Itoh, A. *J. Vac. Sci. Technol. A* **1987**, *5*, 2253.
(7) Kim, K. W.; Hong, C. E.; Choi, S. C.; Cho, S. J.; Whang, C. N.; Shim, T. E.; Lee, D. H. *J. Vac. Sci. Technol. A* **1994**, *12*, 3180.
(8) Maggioni, G.; Carturan, S.; Rigato, V.; Pieri, U. *Nucl. Instr. Methods B* **2000**, *166−167*, 737.
(9) Maggioni, G.; Carturan, S.; Quaranta, A.; Patelli, A.; Della Mea, G. *Chem. Mater.* **2002**, *14*, 4790.
(10) Maggioni, G.; Carturan, S.; Rigato, V.; Della Mea, G. *Surf. Coat. Technol.* **2001**, *142−144*, 156.

10.1021/cm034711i CCC: $27.50
Published on Web 05/20/2004

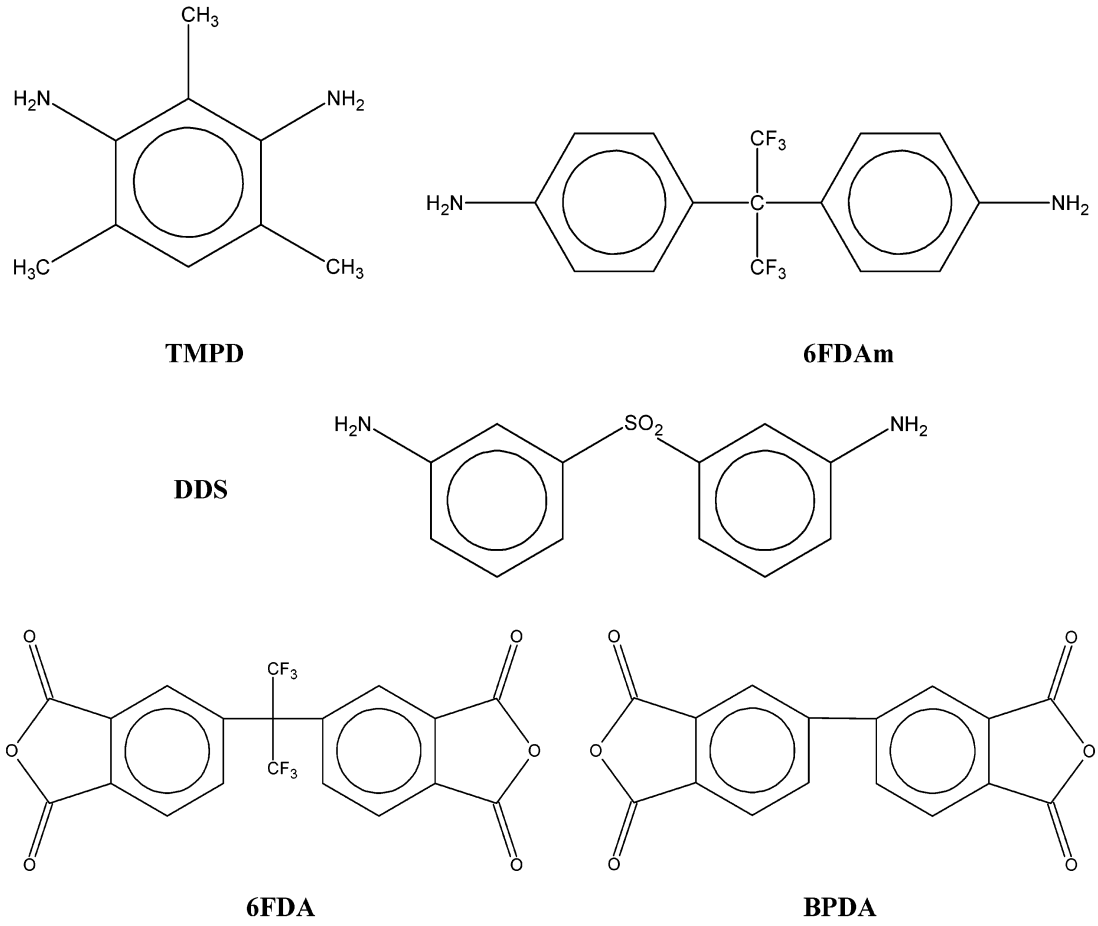

Figure 1. Chemical structure of 2,4,6-trimethyl *m*-phenylenediamine (TMPD), 4,4′-(hexafluoroisopropylidene)dianiline (6FDAm), 3,3′-diaminodiphenyl sulfone (DDS), 4,4′-hexafluoroisopropylidene diphthalic anhydride (6FDA), and 3,3′,4,4′-biphenyltetracarboxylic acid dianhydride (BPDA).

The extension of the GDS method to other polyimides suitable for different applications, such as radiation detector systems, requires a deeper knowledge of the deposition process of the precursor monomers. In particular, the discharge-induced damage, the morphology, and the aggregation state of the different molecules must be investigated to make out the deposition parameters which allow obtention of a homogeneous stoichiometric mixing between the dianhydride and diamine molecules. Moreover, the comprehension of the physical process governing the interaction between a low-energy glow discharge and organic molecules is still relatively unaccomplished, and systematic studies are needed to deepen the knowledge of this process.

In this work we report study of the GDS deposition of five polyimide precursor monomers shown in Figure 1, i.e., 2,4,6 trimethyl *m*-phenylenediamine (TMPD), 4,4′- hexafluoroisopropylidene dianiline (6FDAm), 3,3′-diaminodiphenyl sulfone (DDS), 4,4′-hexafluoroisopropylidene diphthalic anhydride (6FDA), and 3,3′,4,4′-biphenyltetracarboxylic acid dianhydride (BPDA). The choice of the monomers was done taking into account both the final application of the deposited films (i.e., plastic scintillators) and the need of analyzing in detail the correlation between the monomer molecular structure and the final properties of the deposited film. Because the organic network of plastic scintillators must exhibit both radiation hardness and optical transparency to the scintillation light, the monomers were chosen to fulfill these two requirements.

Monomer thin films were also deposited by vacuum evaporation (VE) to compare the GDS method with a traditional deposition technique. The GDS deposition process was characterized by in situ mass spectrometry and by the deposition rate measurement with a quartz crystal microbalance. The surface morphology inspection of the deposited samples was performed via atomic force microscopy (AFM).

FT-IR and fluorescence analyses were performed to study the deposition of integer monomer molecules and the incorporation of molecular fragments in the deposited films. Because the fluorescence properties of the selected organic molecules have not yet been characterized (to the best knowledge of the authors), fluorescence spectroscopy was also performed on liquid samples, prepared by dissolving each chemical species in tetrahydrofuran (THF) at two different concentrations (10^{-2} M and 10^{-4} M).

2. Experimental Section

2.1. Chemicals. The chemical structures of the organic molecules are shown in Figure 1.

TMPD, DDS, and 6FDA were obtained from Lancaster at 99, 98, and 98% purity, respectively; 6FDAm was obtained from Acros Organics at 98% purity; and BPDA was obtained from Acros Chemicals at 97% purity. All the chemicals were used without further purification.

2.2. GDS Apparatus. The experimental equipment used for the glow-discharge deposition of thin organic films consisted of a stainless steel vacuum chamber evacuated by a turbomolecular pump to a base pressure of 10^{-4} Pa. The device used to sustain the glow discharge was a 1-in. cylindrical magnetron sputtering source connected to a radio frequency power generator (600 W, 13.56 MHz) through a matching box. The organic powders were placed on the surface of an aluminum target, and placed on the sputtering source. The amount of precursor monomer used in every deposition was determined so as to always have the same number of molecules on the target, i.e., 1.023×10^{21} (1.7×10^{-3} mol). The only exception was TMPD, which, owing to its low molecular weight, resulted in a very small quantity of powder, so the dose was doubled to ensure complete coverage of the aluminum target. The glow discharge feed gas used in all the depositions was a 95:5 argon/oxygen mixture. The pressure inside the chamber was measured through a capacitance gauge. Typical values of rf power, target DC self-bias, and working pressure were in the ranges 10 to 20 W, −20 to −200 V, and 5.00 ± 0.05 Pa, respectively. A quadrupole mass spectrometer (Hiden Analytical, model PSM 001) was connected to the deposition chamber through an electrically grounded sampling orifice (100-μm diam) and evacuated by a turbomolecular pump to a base pressure of 10^{-6} Pa. For each monomer considered in this work the time evolution of some selected mass-to-charge ratios before, during, and after the deposition was also measured. The selected peaks were at *m*/*z* 16, 18, 20, 28, 32, and 44.

Each monomer was deposited on two substrates simultaneously: the former was a P-doped (100) silicon wafer 350-μm thick lapped on both faces (Atomergic Chemetals Inc.), while the latter was a quartz glass slide (Heraeus Quarzglas GmbH and Co). The substrates were mounted on a rotatable sample holder placed 6 cm above the source. The thickness of the organic layer and the deposition rate were measured in real time by a quartz crystal microbalance.

2.3. Evaporation Apparatus. The experimental equipment used for the evaporation of the organic molecules consisted of a stainless steel vacuum chamber evacuated by a turbomolecular pump to a base pressure of 5×10^{-4} Pa. The powders were placed in a copper crucible that was wrapped with a heating wire.[11] The substrates were placed on a fixed sample holder placed 7.5 cm above the crucible. The deposition rate and film thickness were measured by a quartz microbalance.

2.4. Film Characterization. FT-IR spectra of the samples were recorded in the 4000−400 cm^{-1} range using a Jasco FT-IR 660 Plus spectrometer with a resolution of 4 cm^{-1}. During the measurements, the sample cell and the interferometer were evacuated so as to remove from the spectra the absorption peaks of water and atmospheric gases.

The surface morphology of the samples was inspected by an optical microscope and an atomic force microscope (AFM) model C-21 produced by Danish Micro Engineering, mounting a DualScope Probe Scanner 95-50. The scan size was 2×2 μm^2. All the images were acquired using the AC mode, at a very slow speed, typically under 1 μm/sec.

The thickness of the films was measured by scratching (with a doctor blade) a small area of the samples deposited on silicon and then acquiring an AFM image of the borderline between the exposed substrate and the pristine film.

Emission spectra at room temperature were collected by a Jasco FP-770 spectrofluorometer equipped with a 150-W xenon lamp. The spectral bandwidth was 5 nm for all the spectra. The data were corrected by taking into account the spectral response of the overall detection system (emission monochromator and detection photomultiplier) which was measured by collecting the emission spectrum of a calibrated halogen lamp.

For liquid samples, the 10^{-4} M solutions were prepared to identify the fluorescence emission features of isolated molecules, as their average distance at this concentration is in the order of the tens of nanometers. In contrast, the 10^{-2} M solutions were specifically prepared to spot the formation of fluorescent aggregates which can arise at higher concentrations. Anhydrous tetrahydrofuran (THF) was selected as a solvent because it exhibits a much lower fluorescence with respect to the inspected molecules. Furthermore, owing to its low dielectric constant, the impact of solvatochromic effect on the fluorescence emission of the monomers is limited. In addition, THF is able to dissolve all the considered molecules very well with the exception of BPDA.

UV−visible absorption measurements were performed in the 200−800 nm range using a Jasco V-570 dual-beam spectrophotometer. The spectra were recorded with a resolution of 2 nm.

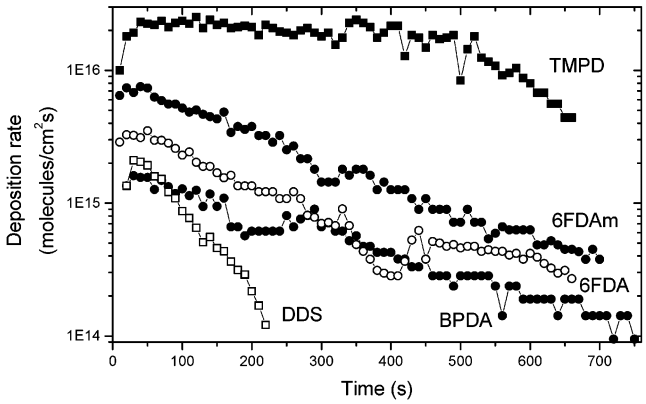

Figure 2. GDS deposition rate of the five monomers as a function of the deposition time.

3. Results and Discussion

3.1. Deposition Rate and Mass Spectrometry. The deposition rate of the monomer molecules is displayed in Figure 2 as a function of deposition time. TMPD monomer displays the highest deposition rate during the whole process. At first it remains nearly constant, decreasing to about 80% the starting value after 500 s; afterward a steeper decay can be observed. On the other hand, the deposition rate of the other monomers follows a nearly exponential decay. The experimental points can be fitted with the following function:

$$\log D = \log D_0 - Bt \qquad (1)$$

where D = deposition rate and t = time. The calculated D_0 and B values are reported in Table 1.

As can be seen from Table 1, the starting deposition rate decreases from 6FDAm to BPDA. On the other hand, the curve slope is comparable for BPDA, 6FDA, and 6FDAm while a much faster decrease is displayed by DDS.

Table 1 also reports the evaporation temperature (T_{evap}) and the evaporation rate in molecules cm^{-2} s^{-1} for each monomer. The evaporation conditions of TMPD do not appear because this powder does not exhibit the usual evaporation behavior; instead, it suddenly "bursts" during the temperature increase without giving rise to any coating on the substrate. No value is shown for the evaporation rate of 6FDA because when its T_{evap} was reached the powder sublimated suddenly and completely.

The time evolution of the GDS deposition rates points out the ion-bombardment-induced damage of the mono-

(11) Maggioni, G.; Carturan, S.; Boscarino, D.; Della Mea, G.; Pieri, U. *Mater. Lett.* **1997**, *32*, 147.

Table 1. Starting Deposition Rate (D_0), Decrease Rate (B), Evaporation Temperature (T_{Evap}), and Evaporation Rate of the Five Monomers

	TMPD	6FDAm	DDS	6FDA	BPDA
D_0 (molecules/cm^{2}s)	2.2×10^{16}	7.9×10^{15}	4.0×10^{15}	3.2×10^{15}	1.6×10^{15}
B (s^{-1})	1.44×10^{-4}	1.96×10^{-3}	6.22×10^{-3}	1.61×10^{-3}	1.54×10^{-3}
T_{evap} (°C)		155	158	205	245
evap rate (molecules/cm^{2}s)		2.2×10^{14}	1.1×10^{14}		1.4×10^{14}

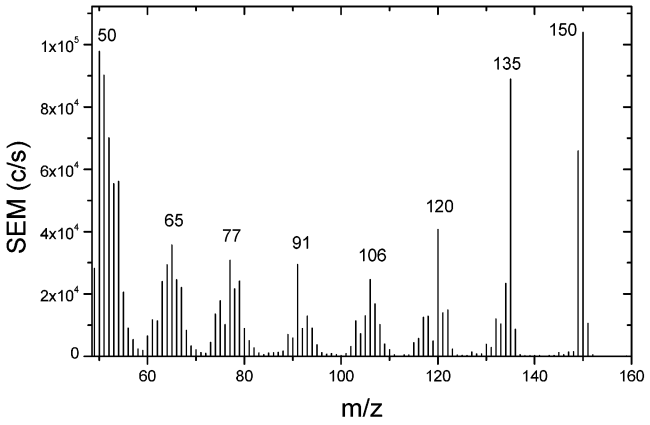

Figure 3. Mass spectrum collected during GDS deposition of TMPD monomer.

mer powder and the formation of a carbon-rich surface layer which hinders further sublimation of integer molecules, as previously reported for the GDS deposition of PMDA and ODA monomers.[8,10] Except for TMPD, the exponential decrease of the deposition rate of all the monomers sets in very quickly, showing the progressive formation of the carbonized layer as highlighted by a gradual color change of the surface powder from white to light brown to dark black after the deposition is completed. FT-IR analysis of the black powder shows the lack of any feature in the whole range (4000−400 cm^{-1}). The exponential decrease indicates that the target damage gives rise mainly to nonvolatile species which cannot be removed from the target surface. The presence of these species, together with the lower starting deposition rates as compared to the one shown by TMPD, gives rise to a faster formation of the carbon-rich layer. This effect is particularly pronounced for DDS, which exhibits the highest decrease rate.

The different behavior of TMPD can be explained by considering the mass spectrum collected during TMPD deposition (Figure 3). The strong molecular ion peak at *m*/*z* 150 shows that the emission of integer monomer molecules takes place. However, comparison with the literature mass spectrum[12] points out that the fragmentation of a significant fraction of the monomer molecules also occurs in the deposition chamber, as pointed out by the high intensity of the fragments peaks (*m*/*z* 135, 122, 118, 107, 91, and 75) as compared to the molecular ion one and by the appearance of some new peaks at *m*/*z* 120, 106, 77, 65, and 50. These features show that the molecular damage induced by the plasma interaction gives rise to the formation of highly volatile phenyl radicals lacking in methyl and amino groups such as 2,*x*-dimethyl-1,3-phenylenediamine (where $x = 4$ or 6), 2,6-toluenediamine, *m*-phenylenediamine, and aniline radicals. The emission of the volatile fragments, together with the strong sublimation of integer TMPD molecules, delays the formation of the carbonized layer, which takes a long time (more than 500 s) compared to the other monomers.

Examining the VE-deposition procedure, it can be seen that three molecules (6FDAm, DDS, and BPDA) follow a similar pattern: once a certain temperature is reached, they undergo a gradual evaporation over a few minutes, with comparable deposition rates. 6FDA and TMPD behave differently: once they reach a critical temperature, they suddenly "burst", evaporating completely in a few seconds. However, 6FDA deposits on the target surface, whereas TMPD does not: this means that the latter molecule undergoes a chemical decomposition on reaching the critical temperature and the molecular fragments do not deposit onto the substrate because they are very volatile, as shown by the mass spectrum collected during the GDS deposition.

By comparing the starting GDS deposition rate (D_0 in Table 1) with the evaporation temperature of the monomers, it is noteworthy that at increasing T_{evap} the starting deposition rate decreases: this trend could be expected because at the early stages of the GDS process the target surface consists of only integer molecules. Therefore, the GD-induced sublimation of the monomers is mainly controlled by thermodynamic factors. Considering the energy lost by the impinging ions is about the same for all the monomers, the sublimation of the most volatile compounds such as TMPD is favored.

As far as the molecular damage is concerned, the analysis of the mass spectra points out the presence of a certain degree of molecular fragmentation for all the monomers (see Supporting Information). In the case of 6FDAm, a very small peak at *m*/*z* 334 (molecular ion) appears in the mass spectrum, together with a fragment peak at *m*/*z* 265, its intensity being comparable to that shown by the molecular ion. In the low mass range (less than *m*/*z* 100) it is possible to spot an intense peak at *m*/*z* 69 (CF_3 group) and two other ones at *m*/*z* 66 (stronger) and *m*/*z* 93 (weaker). The presence of the molecular ion peak in the mass spectrum confirms that part of the 6FDAm molecules are emitted from the target without undergoing damage. However, this feature has a much lower intensity than the one shown by the molecular ion peak of TMPD; this fact indicates that in the gas phase the density of 6FDAm molecules is low in comparison with that of the other monomer, which also exhibits a much higher deposition rate during the whole deposition process. The particularly high intensity of the peak at *m*/*z* 69 together with the presence of the peak at *m*/*z* 265 suggest that the main fragmentation reaction gives rise to the loss of $-CF_3$ groups. This bond cleavage partially occurs in the mass spectrometer, but mostly in the deposition chamber as the relative intensity of the CF_3 peak as compared to the molecular ion one is much higher in the experimental spectrum than in the one shown in the literature.[12] The loss of $-CF_3$

(12) SDBSWeb: http://www.aist.go.jp/RIODB/SDBS/ (accessed May 2003).

groups, which is also found in 6FDA, is due to the low bond strength of $C-CF_3$ as compared to the other chemical bonds in the monomer molecules. On the other hand, the presence of the peaks at *m*/*z* 93 and 66 shows that the damage also can be more severe giving rise to the formation of aniline radicals.

As far as the other monomers are concerned, the analysis of the mass spectra does not give any information about the sublimation of undamaged molecules from the target. This fact is due to the low deposition rate of these monomers as compared to those of 6FDAm and TMPD. Actually, whereas the deposition rate of 6FDAm is high enough to enable the detection of undamaged molecules during the first part of the deposition process, this does not occur for the other monomers, whose deposition rates are much smaller and below the detection limit of the instrument during the whole process.

For DDS some peaks can be identified at *m*/*z* 93, 76, 66, 64, and 51 (see Supporting Information). In particular, the peak at *m*/*z* 64, which is the most intense one, is assigned to the SO_2 group. Similarly to the $-CF_3$ group in 6FDAm and 6FDA, the loss of SO_2 occurs owing to the weak bond between this group and the rest of the molecule. The aniline molecule and its related radicals also can be spotted from the peaks at *m*/*z* 93 and 66, while benzene and its fragments are identified owing to the signals placed at *m*/*z* 76 and 51.

In the dianhydrides spectra, the CO and CO_2 peaks appear, mainly arising from the molecular fragmentation of the five-membered anhydride rings as previously reported for pyromellitic dianhydride (PMDA) deposition.[10]

The measurement of the time evolution of some selected peaks (i.e., at *m*/*z* 16, 18, 20, 28, 32, and 44) during the monomer deposition (see Supporting Information) throws some light on the role of the molecular oxygen added to the plasma atmosphere. Oxygen-containing plasmas are widely used to strip hydrogenated carbon films by converting the C_xH_y-based species to volatile products.[13] As a matter of fact, gaseous oxygen can react with the carbonaceous species hindering the sublimation of the monomer molecules from the target surface and the resulting effect is the emission of volatile species such as CO and CO_2. During the deposition of all the monomers an increase of the CO (*m*/*z* 28) and CO_2 (*m*/*z* 44) peaks and a decrease of the O_2 peak (*m*/*z* 32) can be observed after the plasma ignition. On the other hand, the atomic oxygen peak at *m*/*z* 16 shows neither an increase as the plasma is ignited nor a decrease when the plasma is turned off, but it follows the behavior of the water peak (*m*/*z* 18), which is plasma-insensitive, as well as the peak at *m*/*z* 20, which is mostly due to Ar^{2+}. Because an increase of the atomic oxygen peak could be expected after the plasma ignition owing to the dissociation of molecular oxygen, it can be deduced that the atomic oxygen present in the deposition chamber reacts with the carbon-rich layer giving rise to the formation of the CO_x species, while the water dissociation in the mass spectrometer mainly contributes to the peak at *m*/*z* 16. It is worth noting that in the case of dianhydrides the emission of CO_x molecules is also due to the fragmentation of the five-membered anhydride groups of 6FDA and BPDA, as observed above.

(13) Alves, M. A. R.; da Silva Braga, E.; Fissore, A.; Cescato, L. *Vacuum* **1998**, *49*, 213.

Table 2. Thickness, Average Roughness, and Lateral Dimension of Surface Islands of the VE and GDS Films as Measured by AFM

	thickness (nm)	roughness (nm)	lateral dimension (nm)
	GDS films		
TMPD	445	4.6	8000
6FDAm	375	0.4	100
DDS	88	1.1	200
6FDA	885	57	750
BPDA	157	0.6	180
	VE films		
6FDAm	2310	33	850
DDS	592	14	220
6FDA	1640	0.3	350
BPDA	769	13	600

3.2. Morphology of the Deposited Films. The average roughness, calculated on a 2 μm × 2 μm area, and the thickness of both GDS and VE films as determined by AFM are reported in Table 2.

The optical inspection of the deposited samples shows that the VE films are white and opaque, whereas the GDS ones appear light yellow and transparent. Moreover, the presence of big, isolated, powdery grains is found in both the GDS-deposited TMPD sample and of the VE-deposited 6FDA sample. The AFM images of these latter samples were acquired in a relatively smooth region far from these grains in order to avoid damaging the microscope tip.

The average roughness of the deposited films ranges from <1 nm to some tens of nm, but the surface morphology of both VE and GDS samples consists of islands of several hundreds of nm of lateral dimension, as reported in the last column of Table 2. VE samples exhibit a higher roughness with respect to the GDS samples, as shown in Figure 4 for BPDA thin films (see also Supporting Information).

Some considerations on the growth mode of the deposited films can be drawn from these results. GDS-deposited TMPD and VE-deposited 6FDA films appear rough and powdery compared to the other samples due to the incorporation of grains visible to the naked eye that are emitted during the deposition process together with the sublimated single molecules. As to the other monomers, the lower roughness and the smaller lateral dimensions of the morphological features appearing in the GDS films as compared to the ones shown by the VE samples suggest different growth modes in the two deposition processes as arising from the different average energy of the monomer molecules in the two processes. The average energy of the GD-sublimated molecules impinging on the substrate can be estimated to be some eVs. This value is calculated by considering that in a previous work it has been shown that most sublimated molecules acquire a positive electrical charge because they are either protonated (dianhydrides) or ionized (dianhydrides and dianilines) during their fly from the target to the substrate.[10] This means that when passing through the plasma/substrate sheath the ionized molecules can acquire enough energy to react easily with the silicon surface, giving rise to a high

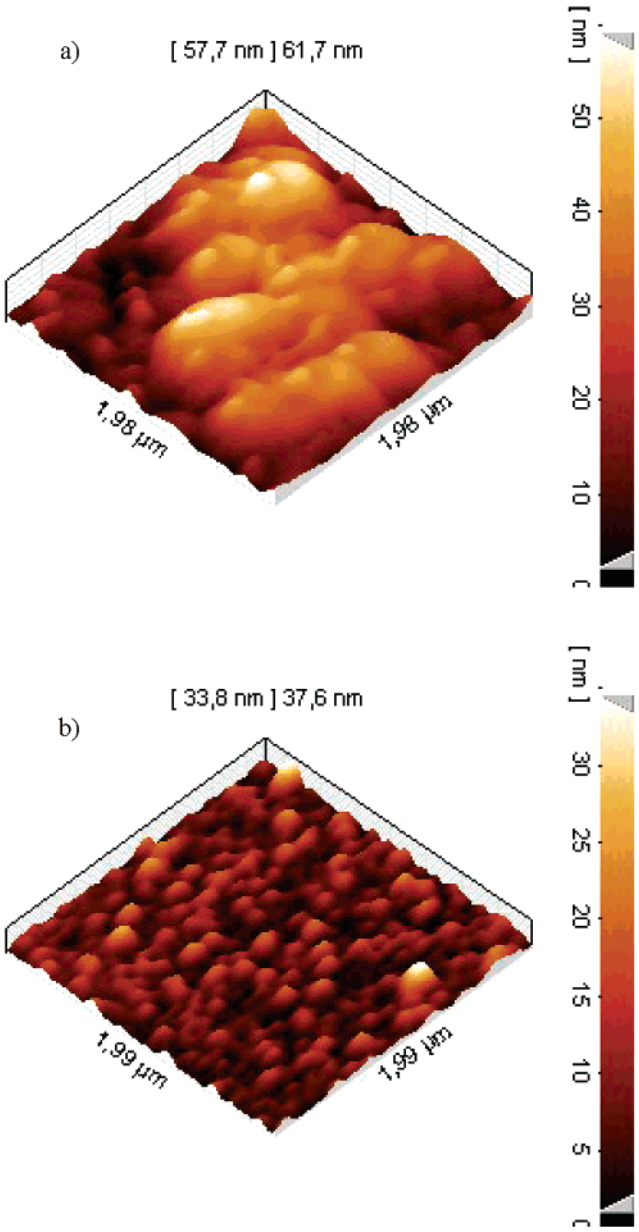

Figure 4. AFM images of (a) VE-deposited and (b) GDS-deposited BPDA films.

density of nucleation sites on the surface, thus promoting the growth of several small grains.

On the other hand, during the evaporation process the average energy of the monomer molecules is lower than one eV (thermal energy) and they can mainly interact with the hydrolyzed sites of the silicon surface (silanol groups, Si−OH). Because the density of nucleation sites is lower, the growth of fewer but bigger grains is promoted.

A seemingly anomalous behavior is observed in the case of 6FDA: the roughness and the lateral dimensions of the morphological features appearing in the GDS film are very pronounced, whereas the VE film exhibits a very low roughness. As far as the GDS film is concerned, the reason for this difference is not clear at the moment, whereas for the VE sample it must be taken into account that large grains visible to the naked eye are present due to the very peculiar evaporation mode (i.e., complete evaporation within few seconds). Hence, the effective

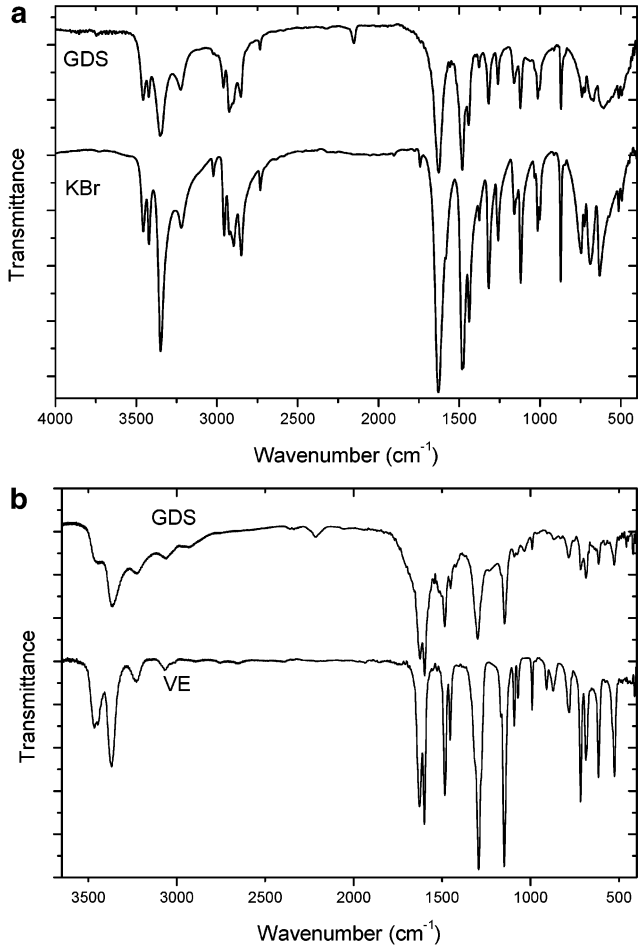

Figure 5. FT-IR spectra of (a) TMPD powder in KBr pellet (lower) and GDS-deposited TMPD thin film (upper); and (b) VE-deposited (lower) and GDS-deposited (upper) DDS films.

average roughness is much higher than that measured by AFM.

3.3. Spectroscopic Characterization of the Deposited Monomers. Taking into account that several molecular fragments due to the monomer damage were observed by mass spectrometry during the deposition of all the monomers, a first inspection on the degree of damage in the deposited films can be done by means of FT-IR spectroscopy.

All the FT-IR spectra of VE- and GDS-deposited samples were compared with the ones of the corresponding monomer powders in KBr pellets. In Figure 5a are reported the spectra of the TMPD GDS-deposited sample and of the KBr-pelletized monomer; the spectrum of the VE sample does not appear because the evaporation of this monomer was unsuccessful, as already outlined. As can be seen, all the main characteristic peaks appear in the spectrum of the GDS-deposited film, showing that the deposition of integer molecules has been performed. The position and the relative intensity of the peaks in the 3000−3500 cm^{-1} region (N−H stretching) are the same in both spectra. As far as the methyl group peaks are concerned (region 3000−2700 cm^{-1}), the position is the same but the relative intensity is slightly different. Although all the main peaks appear in the fingerprint region (1800−700 cm^{-1}), their position is translated to lower wavenumbers with respect to the reference spectrum. As far as the

inclusion of molecular fragments is concerned, a comparison of both GDS and KBr FT-IR spectra with those reported in the literature for aniline and *m*-phenylenediamine[12] shows that a significant incorporation of these molecules in the film has to be excluded because their typical IR features, which do not overlap the ones characterizing TMPD, are not clearly evident. As far as 2,6-toluenediamine and 2,*x*-dimethyl-1,3-phenylenediamine radicals ($x = 4$ or 6), whose presence in the deposition atmosphere is shown by the peak groups around 120 and 135 *m*/*z* in the mass spectrum, respectively, the typical IR features of both molecules cannot be resolved from the ones characterizing the TMPD. Hence, their incorporation in the film cannot be excluded, especially considering that the melting point of these species is comparable to the one characterizing TMPD. The only clear evidence of the presence of molecular fragments in the GDS film comes from the presence of the weak absorption at 2160 cm^{-1}, which does not appear in the TMPD powder. This peak is ascribed to the C≡C stretching, arising from the phenyl ring opening.

Similarly to TMPD, the IR spectra of the other monomers (see Supporting Information) show all the main characteristic features of the selected molecules, showing that the sublimation and the deposition of integer molecules has been obtained in all the cases.

In the case of DDS (Figure 5b), the inclusion of molecular fragments into the GDS film is evidenced by the presence of the small peak at 2210 cm^{-1}, which was assigned to C≡N stretching, and by the low intensity of the SO_2 group peaks at 1295 and 1150 cm^{-1} (stretching C−SO_2−C) as compared to the peaks at 1600 and 1625 cm^{-1}. This last feature indicates a partial lack of SO_2 groups in the film, as to confirm the mass spectrometry findings, which pointed out a strong presence of SO_2 in the deposition atmosphere.

In the case of the other GDS-deposited monomers, FT-IR spectra do not clearly show the presence of molecular fragments in the films, although mass spectrometry points out the presence of CF_3 groups (in the 6FDA and 6FDAm deposition) and CO_x species (in the 6FDA and BPDA deposition). This seeming discrepancy can be explained in different ways: (i) the molecular fragments are incorporated in the film but their IR peaks cannot be discriminated from the ones shown by the monomers (similarly to TMPD); (ii) the molecular fragments are volatile species and are not incorporated in the film; or (iii) the molecular fragmentation takes place mainly on the target and only low-mass, highly volatile fragments such as CF_3 and CO_x groups can escape from the target while the remaining parts of the damaged monomers cannot sublimate, thus giving rise to the carbonized surface layer.

FT-IR analysis also shows a certain degree of structural disorder in all the GDS films; as a matter of fact, by comparing height and width of the IR peaks of GDS and VE films, a band broadening is observed in all the GDS samples, even if less evident in the case of BPDA. The broadening is particularly pronounced for the high-wavenumber peaks such as those originating from the stretching of C−H and N−H bonds. This could be expected because C−H and N−H bonds are located on the outer edges of the various molecules and therefore are particularly susceptible to their chemical surroundings.[14] Even a slight difference in the chemical environment produces a distinct distortion of the molecular structure; the electric dipole moment of the single molecule changes significantly owing to the relatively high partial charges placed on the considered atoms. This results in a visible shift of the transition frequency of that particular molecule in the IR range.[15,16] Therefore, each different chemical environment produces a slightly different transition frequency, thus resulting in the overall broadening of the IR band. As far as the backbone carbon atoms are concerned, their partial charges are much smaller, therefore the variation of dipole moment produced by a slight molecular deformation is limited. Moreover, most carbon-to-carbon bonds are present in rigid aromatic rings, so that they are energy-stabilized as compared to the C−H and N−H bonds and much more difficult to distort. The minimal broadening of the C═O band can be also explained as described above; as a matter of fact the rigid five-membered anhydride ring effectively opposes the distortion, thus reducing the effects of the chemical environment on the C═O infrared features. Furthermore, the lower broadening of the BPDA peaks as compared to the other monomers is maybe due to the higher rigidity of its molecular structure.

In the analysis of the deposited monomer film structure optical spectroscopy plays an important role as it mainly deals with the delocalized molecular orbitals of the aromatic groups. Therefore, fluorescence spectroscopy can be exploited to investigate both the damage degree of the molecule and its chemical surroundings. Table 3 reports the peak wavelengths of the fluorescence features observed for monomers dispersed in THF (10^{-4} and 10^{-2} M) and for the corresponding VE- and GDS-deposited samples. The fluorescence analysis of the monomers dispersed in THF allows identification of the emission features of single molecules and/or aggregates, so that any different peak can be ascribed to some kind of molecular fragment. Under ultraviolet excitation all the THF-dissolved monomers exhibit an emission peak at a wavelength ranging from 312 to 385 nm in the 10^{-4} M solution. Semiempirical calculations performed by MOPAC 2000[17] show that this feature can be ascribed to the isolated single monomer emission; this result could be expected by taking into account that the average distance between the molecules at this concentration is in the order of the tens of nm. On the other hand, except for DDS, some further peaks are identified at higher wavelengths (ranging from 380 to 435 nm), which can be ascribed to dimers and/or higher size aggregates. At increasing concentration the fluorescence of the aggregates is promoted but the emission of the single molecules still takes place, except for the 6FDA monomer. In particular the monomer and dimer emissions of BPDA are slightly shifted to higher wavelengths.

The presence of the monomer peaks in the more concentrated solution suggests that the emission features of the solid state monomers in the films should

(14) Heitz, T.; Drevillon, B.; Godet, C. *Phys. Rev. B* **1998**, *58*, 13957.
(15) Mahan, G. D.; Lucas, A. A. *J. Chem. Phys.* **1978**, *68*, 1344.
(16) Person, B. N. J.; Rydberg, R. *Phys. Rev. B* **1981**, *24*, 6954.
(17) *MOPAC 2000*. Stewart, J. J. P.; Fujitsu Limited: Tokyo, Japan, 1999.

Table 3. Fluorescence Peaks Observed for the Different Monomer Samples

	THF (10^{-4} M)		THF (10^{-2} M)		VE		GDS	
monomer	λ_{ex} (nm)	λ_{em} (nm)	λ_{ex} (nm)	λ_{em} (nm)	λ_{ex} (nm)	λ_{em} (nm)	λ_{ex} (nm)	λ_{em} (nm)
TMPD			320	**340** (monomer)				
	260	**335** (monomer)	360	**415** (dimer)			300	490
	345	**415** (dimer)	400	**475** (aggregates)				
6FDAm	300	**330** (monomer)	320	**335** (monomer)	280	**330** (monomer)	350	500
	365	**420** (dimer−aggregates)	355	**420** (dimer−aggregates)	350	**530** (very faint)	350	**580** (shoulder)
					280	**345** (monomer)		
DDS	345	**385** (monomer)	360	**385** (monomer)	350	**372** (monomer in more polar environment)	300	440
6FDA	270	**312** (monomer)	330	**415** (aggregates)	275	**322** (monomer)	300	580
	320	**380** (dimer−aggregates)			305	**500** (aggregates)		
BPDA	335	**357** (monomer)	335	**370** (monomer)	315	**362** (monomer)	330	**360** (monomer)
	345	**435** (dimer)	370	**444** (dimer)				

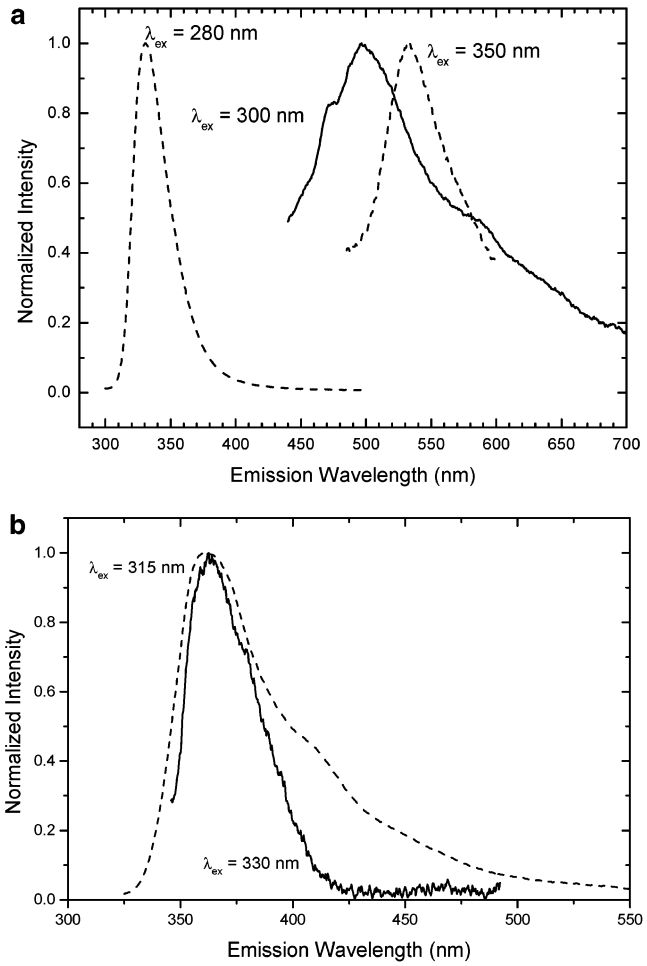

Figure 6. Emission spectra of (a) VE-deposited (- - -) and GDS-deposited (−) 6FDAm thin films; and (b) VE (- - -) and GDS (−) BPDA thin films. The excitation wavelengths are indicated.

be maintained and this is true for the VE films which show the characteristic emission of the single molecules as observed in the THF solutions (Figure 6 and Supporting Information). In the case of 6FDA the monomer peak is shifted to 322 nm, maybe indicating that the molecule is embedded in a more polar environment. The different environment polarity also explains the fluorescence peak at 372 nm which appears in the VE-deposited DDS film under excitation at 350 nm. By exciting the VE deposited samples at different wavelength, only 6FDA and 6FDAm exhibit new fluorescence bands, which cannot be assigned to dimers owing to their noticeable shift with respect to the bands observed in the higher concentration solution. This new feature is probably due to the presence of damaged molecules owing to the more pronounced fragility of this kind of molecules caused by the presence of the labile $C(CF_3)_2-$ group. On the other hand, it is worth noting that in the case of VE 6FDA films the emission from the single molecule can be clearly observed, whereas it was not visible in the more concentrated solution, as stated above. This fact can be ascribed to the very high evaporation rate of 6FDA and to its effects on the mobility of the condensed molecules: as a matter of fact, the dissolved monomer molecules can easily move and form aggregates. In contrast, during the evaporation of 6FDA, which lasts just a few seconds, the growth of the film is so fast that the condensed molecules are frozen in their positions and can neither move nor rotate to find the minimal energy configuration typical of an aggregate of two or more molecules.

As far as the GDS samples are concerned, the fluorescence bands lie at longer wavelengths with respect to VE samples and do not exhibit features which can be attributed to single molecules, except for BPDA (Figure 6 and Supporting Information). The TMPD film exhibits a faint peak at 490 nm which is assigned to some kind of aggregate similar to that found in the most concentrated solution (peak at 475 nm). On the other hand, the emission features of 6FDAm, DDS, and 6FDA films can be ascribed neither to single molecules nor to aggregates. Taking into account the findings of mass spectrometry and FT-IR analysis, this behavior can be explained by assuming that these samples contain three kinds of molecular species: (i) integer monomer molecules; (ii) severely damaged molecules, with at least one aromatic ring opened (producing the C≡C and C≡N IR peaks); and (iii) weakly damaged molecules, probably differing from the undamaged ones by just one or a few lacking hydrogen atoms of an aromatic ring. Once they reach the substrate during the film deposition, the weakly damaged molecules react with the integer ones or with themselves, thus forming disordered aggregates with a wider delocalization of the optically active orbitals. The structural difference between integer and weakly damaged molecules is too small to be detected by FT-IR analysis, but their fluorescence features are very different from the integer

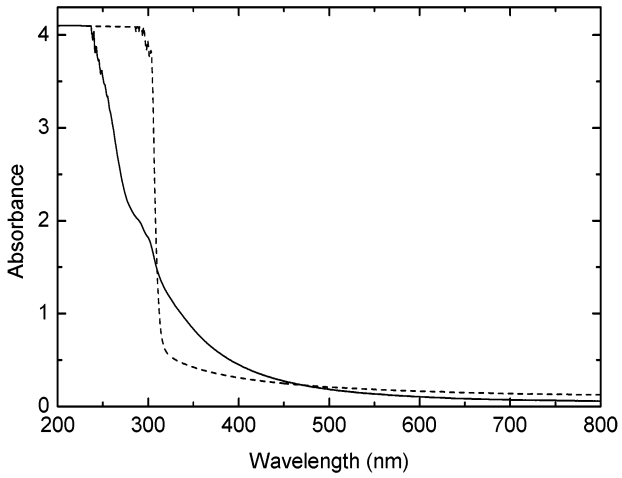

Figure 7. UV−vis absorption spectra of VE-deposited (- - -) and GDS-deposited (−) 6FDA thin films.

molecules and very similar to hydrogenated amorphous carbon clusters (*a*-C:H): in fact, the latter ones show a distinct luminescence emission at wavelengths greater than 500 nm.[18−20] The basic structure of the *a*-C:H clusters consists of a mixture of carbon atoms with different hybridizations (either sp^2 or sp^3),[18−21] probably islands of sp^2-hybridized atoms enclosed in a sp^3 matrix, so as to relieve strain.[18,22] The weakly damaged molecules are similar to *a*-C:H because all the starting monomers are aromatic (sp^2 carbons) and also contain sp^3 carbons. The delocalization of the optically active orbitals in the weakly damaged molecules results in an absorbance in the visible region as shown by the UV−vis absorption spectra (Figure 7). The absorption tail of the GDS films accounts for their characteristic light yellow color. The monomer excited states can be then quenched either by nonradiative decay paths or can transfer their excitation energy to the (*a*-C:H)-like systems, thus resulting in the long-wavelength emission. The presence of aggregates of weakly damaged molecules also explains the high wavelength emission shown by 6FDA and 6FDAm in the VE samples. It is worth noting the different origin of the absorption tail in the case of VE films (see Figure 7): it arises from a scattering effect which accounts for their typical white color.

The only exception is the fluorescence emission of the GDS-deposited film of DDS. In this case a faint, broad band at about 440 nm can be observed, at a lower wavelength than the usual fluorescence features observed in the *a*-C:H systems. For the moment, the assignment of this band is not clear, but because a high degree of damage was detected in this film, mainly involving the loss of the SO_2 groups, it can be inferred that the observed fluorescence band is due to the molecular fragments resulting from this bond breaking.

Among the GDS samples, BPDA is the only monomer that shows the fluorescence peak of the isolated integer molecule. This fact probably indicates that a high structural rigidity somehow inhibits the formation of the aggregates of damaged molecules. As previously observed this rigidity gave rise also to a lower broadening of the IR peaks of this monomer. In a previous work[9] the 3-hydroxyflavone dye molecule was deposited using the GDS procedure as an integer molecule and it preserved its optical properties. Therefore, it can be concluded that some molecules, probably those characterized by a rigid structure, can be deposited via GDS to obtain films sharing the same optical properties as those of the isolated molecules.

4. Conclusions

Thin films of different polyimide precursor monomers have been deposited by means of the novel glow-discharge-induced sublimation procedure. The deposition rate of all the monomers decreases with time owing to the formation of a carbonaceous layer on the powder target surface which hinders further molecule sublimation. The time evolution of the deposition rate is related to the damage of the different molecules: when the ion bombardment of the target monomer gives rise to highly volatile compounds, such as in the case of TMPD, the decrease of the deposition rate is delayed. On the other hand, the presence of labile groups, such as SO_2 in DDS and $C(CF_3)_2$− in 6FDA and 6FDAm, promotes the molecular damage and the production of nonvolatile species, thus leading to a fast decrease of the deposition rate.

Mass spectrometry shows that the ion bombardment of the monomer powders gives rise to the sublimation of integer monomer molecules in the case of TMPD and 6FDAm. Fragmentation of the monomer molecules also occurs due to both the ion bombardment of the target and the gas-phase reactions of the sublimated molecules.

Concerning the film growth process, more homogeneous and flat films can be produced by GDS with respect to the standard vacuum evaporation, owing to the high energy and reactivity of plasma sublimated organic molecules. Moreover, in some cases, such as TMPD and 6FDA, the GDS procedure allows better control of the deposition process.

From the analysis of FT-IR spectra it can be deduced that the deposited films consist of undamaged molecules with some partially damaged species. On the other hand, UV−Vis spectroscopy analysis shows that the GDS deposition gives rise to the formation of molecular structures with optical properties different from those of the starting monomers. This effect can be ascribed to both the higher energy of the impinging monomer molecules and the presence of damaged structures which form different kinds of optically active aggregates. The only exception is BPDA, which exhibits the typical monomer fluorescence features, indicating that it preserves its molecular structure also from the point of view of the electronic molecular orbitals. This peculiarity is ascribed to the higher rigidity of this molecule as compared to that of the other selected monomers.

The results of the present work allow two final conclusions in view of the deposition of fluorescent polyimide coatings by means of the GDS method: (i) the monomers characterized by a rigid structure (e.g., BPDA) can be deposited by adopting the same deposi-

(18) Rusli; Robertson, J.; Amaratunga, G. A. J. *J. Appl. Phys.* **1996**, *80*, 2998.
(19) Pascual, E.; Serra, C.; Bertan, E. *J. Appl. Phys.* **1991**, *70*, 5119.
(20) Smith, F. W. *J. Appl. Phys.* **1984**, *55*, 764.
(21) Franchini, G.; Paret, V.; Tagliaferro, A.; Thèye, M.-L. *J. Non-Cryst. Solids* **2002**, *299−302*, 858.
(22) Robertson, J.; O'Reilly, E. P. *Phys. Rev. B* **1987**, *35*, 2946.

tion parameters used in this work; but, (ii) flexible monomers with labile substituent groups require further experimental work before their use in GDS deposition to ensure a lower molecular damage thus preserving the original fluorescence features.

Acknowledgment. This research was financially supported by the Fifth Commission of Istituto Nazionale di Fisica Nucleare (ASTHICO project).

Supporting Information Available: Mass spectra collected during GDS deposition of 6FDAm, DDS, 6FDA, and BPDA monomers; time evolution of some selected mass peaks during the GDS deposition; AFM images of TMPD, 6FDAm, DDS, and 6FDA films; FT-IR spectra of 6FDAm, 6FDA, and BPDA films; and emission spectra of TMPD, DDS, and 6FDA films (pdf). This material is available free of charge via the Internet at http://pubs.acs.org.

CM034711I